

000 MIND THE BUDGET: ACCELERATING DEEP REIN- 001 FORCEMENT LEARNING USING EARLY EXIT NEURAL 002 NETWORKS 003

004 **Anonymous authors**
 005
 006

007 Paper under double-blind review
 008
 009

010 ABSTRACT 011

012 The "*Bitter Lesson*" from Richard S. Sutton emphasizes that AI methods leveraging
 013 computation tend to outperform those relying on human insight, underscoring
 014 the value of approaches that use computational resources efficiently. In deep rein-
 015 forcement learning (DRL), this highlights the importance of reducing both training
 016 and inference time. While early exit neural networks, models that adapt computa-
 017 tion to input complexity, have proven effective in supervised learning, their use in
 018 DRL remains largely unexplored. In this paper, we propose the use of Budgeted
 019 EXit Actor (**BEXA**), which is a novel actor-critic architecture that integrates early
 020 exit branches into the actor network. These branches are trained via the underly-
 021 ing DRL method and use a constrained value-based criterion to decide when to
 022 exit, allowing the policy to dynamically adjust its computation. **BEXA** is general,
 023 easy to tune and compatible with any off-policy actor-critic method. We evaluate
 024 **BEXA** using different DRL methods such as SAC and TD3 on a suite of MuJoCo
 025 tasks. Our results demonstrate a substantial improvement in inference efficiency
 026 with minimal or no loss in performance. These findings highlight early exits as a
 027 promising direction for improving computational efficiency in DRL.
 028
 029

030 1 INTRODUCTION 031

032 Recent work has demonstrated favorable scaling properties of large neural networks (NNs) in deep
 033 reinforcement learning (DRL), (Farebrother et al., 2024; Nauman et al., 2024; Obando-Ceron et al.,
 034 2024). However, increasing network depth leads to higher computational costs, making DRL more
 035 expensive to train and more difficult to deploy. This is particularly problematic in areas such as
 036 robotics, where budget constraints on the inference time must be satisfied. Current methods in DRL
 037 try to speed up inference by using model compression techniques like neural network pruning and
 038 quantization, reducing the number of model computations while maintaining performance (Zhang
 039 et al., 2023). Yet, these methods can be hard to tune and might lead to potential training overhead.

040 Importantly, a lot of compression methods fail to leverage an inherent property of function approx-
 041 imation in DRL: the computational complexity required for selecting an optimal action varies with
 042 the state. For illustration, in chess, finding the best move depends on the complexity of the position.
 043 Some positions allow for quick detection of strong moves, while others require extensive computa-
 044 tion. Thus, in DRL, where the policy is a neural network, we face a challenge: traditional neural
 045 networks are static, performing the same computations regardless of the input. This can lead to
 046 inefficiency, since for some inputs an action could be derived with significantly fewer computations.

047 Early exit neural networks (ENNs) are dynamic NNs that adapt their computational graph based
 048 on the input. Originating in fields with high computational demand like computer vision (CV)
 049 (Laskaridis et al., 2021) and natural language processing (NLP) (Xu & McAuley, 2023), they work
 050 by adding side branches to the network, so-called exits. A gating mechanism decides on which exit
 051 to take, adaptively controlling the network depth, enabling a trade-off between performance and
 052 efficiency, and potentially improving generalization and interpretability (Han et al., 2022). In many
 053 CV and NLP tasks, they have achieved performance comparable to that of their static counterparts
 while using only a fraction of floating point operations (FLOPs).

Despite their advantages, dynamic neural networks like ENNs have been hardly explored in reinforcement learning (RL). A partial explanation is that naively applying such networks to RL is not possible, as RL has some unique aspects compared to supervised learning. One of the biggest challenges is the lack of supervision, as the agent has to find the correct actions on its own. Typically, early exit branches are trained directly on fixed ground truth data, whereas in RL the behavior of the agent changes over time. In addition, the predicted actions influence the state distribution encountered by the agent. Poorly chosen actions of ENNs can therefore lead to learning instabilities.

In this work, we systematically investigate how to transfer ENNs into DRL. Based on our findings, we propose a new method called Budgeted EXit Actor (**BEXA**), which introduces early exit NNs with resource-constrained gating based on Q-values to speed up policy inference time during training and evaluation. Our main contributions are as follows:

1. We present **BEXA**, a general off-policy actor-critic method, with careful adjustments for using ENNs effectively in DRL for reducing the number of required FLOPs during training and deployment.
2. A novel, budget-aware gating mechanism that selects early exits optimally via a linear program, directly balancing expected return and computational cost.
3. We conduct extensive ablation studies to evaluate different design choices for early exit networks in actor-critic methdos.
4. We benchmark our method on well-known DRL methods such as SAC (Haarnoja et al., 2018) and TD3 (Fujimoto et al., 2018) and show the effectiveness of our method on different MuJoCo tasks.

2 RELATED WORK

We divide related work into two categories: (i) early exit neural networks (ENNs), which have been primarily explored in domains outside of deep reinforcement learning (DRL), and (ii) methods for accelerating training and inference in DRL, such as model compression and software optimization. Within the second category, we also highlight the few approaches that combine both directions in a manner similar to our work.

2.1 EARLY EXIT NEURAL NETWORKS

Early exit neural networks (ENNs) belong to the family of dynamic neural networks (NNs). These are models that change their computational graph based on the input they receive (Han et al., 2021). Some instances adjust their depth using early exits, while others adjust their width by changing the number of neurons or channels in each layer, or by changing their parameters. We focus on early exit networks because they are conceptually straightforward and have been extensively studied (Scardapane et al., 2020b). Here, we will present only a few noteworthy works and refer the interested reader to comprehensive surveys (Laskaridis et al., 2021; Xu & McAuley, 2023; P et al., 2025).

The first works for these networks include conditional deep learning network (CDLN) (Panda et al., 2016) and BranchyNet (Teerapittayanon et al., 2016). CDLN first trains the backbone network and then adds linear early exits at multiple depths, retaining only those that improve performance. BranchyNet integrates exits into known computer vision (CV) classifier networks and uses an entropy-based criterion to terminate computation early. All exits are trained jointly with a weighted cross-entropy loss. While effective in CV, such entropy criteria are not directly applicable to DRL, where high policy entropy is beneficial for exploration.

More recent work goes beyond simple entropy-based criteria with alternative decision rules. Confidence to exit can be defined by maximum class probability (Huang et al., 2018; Wang et al., 2022) or by patience, exiting when several consecutive branches agree (Zhou et al., 2020; Zhu, 2021), a strategy common in early exit transformers. Beyond heuristics, the decision to exit can also be learned: Demir & Akbas (2024) jointly optimizes accuracy and efficiency to train exits and gates, while Vashist et al. (2022) uses DRL to learn an exit policy using a deep Q-network (DQN), though the underlying task is not a DRL one. The work presented here, can be seen as an extension to tuning the exit selection process with DRL. However, rather than learning gate decisions with reinforcement

learning (RL), we formulate exit selection as a resource allocation problem: value estimates from DRL are optimized under a budget constraint via a linear program, which supervises gate policy learning.

Training strategies can also vary. The most common approach is to jointly optimize all exits under a combined loss (Berestizshevsky & Even, 2019; Scardapane et al., 2020a). However, the modular design of early exits also allows for a layer-wise training scheme (Hettinger et al., 2017), where a subset of exits is trained at a time while keeping the rest frozen.

Finally, self-distillation (Zhang et al., 2019) is a variant of knowledge distillation in which knowledge is transferred from a teacher model to one or more student models. Applied to an ENN, the final output layer can be considered the teacher, while the intermediate outputs are the students. These outputs are trained using a combination of a standard supervised loss and an additional imitation loss that encourages the outputs to mimic the teacher’s predictions. Previous work has shown that self-distillation can improve model accuracy (Zhang et al., 2022; Pham et al., 2022), and its self-imitation perspective makes it a natural asset for DRL transfer.

2.2 ACCELERATING DRL

Two directions have emerged for accelerating training and inference in DRL. The first targets system-level efficiency through software and hardware optimizations, such as parallelization and the use of accelerators like GPUs. The second approach focuses on model-level efficiency, compressing neural networks that represent policies, value functions and dynamics models.

On the system side, Weng et al. (2022) parallelizes environment simulation with a C++ backend, reducing Python overhead and enabling high-throughput sampling. We adopt this setup in our experiments as well. Pushing this further, Dalton & Frosio (2020) ports Atari to the GPU, yielding even faster parallel roll-outs. Architecturally, IMPALA (Espeholt et al., 2018) decouples acting from learning by running environments in separate processes, each with its own policy, and asynchronously aggregates experience into a shared buffer. SEED RL (Espeholt et al., 2019) refines this design by batching observations from many environments and evaluating a single policy on an accelerator throughout training.

On the model side, NN compression techniques such as quantization (Nagel et al., 2021), knowledge distillation (Hinton et al., 2015), and pruning (LeCun et al., 1989) have proven highly effective in supervised learning for improving runtime. Recent works adapt these techniques to DRL. QuaRL (Krishnan et al., 2022) quantizes policy parameters after each update from 32-bit floating point to 8-bit integers, improving throughput with minimal accuracy loss. FastAct (Zhang et al., 2023) generalizes this idea by supporting arbitrary compression schemes, while a scheduler ensures that compression remains within acceptable limits to maintain performance.

One closely related line of work is RAPID-RL (Kosta et al., 2022), which integrates early exit networks into DQN. It estimates confidence by checking whether an exit’s Q-value exceeds a fixed fraction of the maximum Q-value, employs layer-wise training, and reports faster inference on Atari. Our approach differs in three key aspects: (i) we target general actor-critic methods rather than DQN, requiring early exits only for the actor and permitting more flexible critic architectures, (ii) we introduce a novel resource-aware early exit criterion and train it jointly with all exits, and (iii) whereas RAPID-RL primarily reduces deployment-time inference but incurs training overhead by evaluating all exits, our method accelerates both training and inference.

3 PRELIMINARIES

Reinforcement learning (RL) problems are commonly formulated as Markov decision processes (MDPs). An MDP consists of an agent interacting with an environment, where the agent follows a policy $\pi(a | s)$ that determines the next action given a state s . At each time step t , the agent chooses an action a_t that is executed in the environment, which, in response, returns the next state $s_{t+1} \sim P(s_{t+1} | s_t, a_t)$ according to the transition probability function P . Additionally, the agent receives a reward $r_t = R(s_t, a_t) \in \mathbb{R}$, where R is the reward function. This reward is a scalar value that describes the desirability of the given state and the chosen action. The cumulative sum of rewards, known as the return, is defined as $G_t = \sum_{k=0}^{\infty} \gamma^k r_{t+k}$ where $\gamma \in [0, 1]$ is the dis-

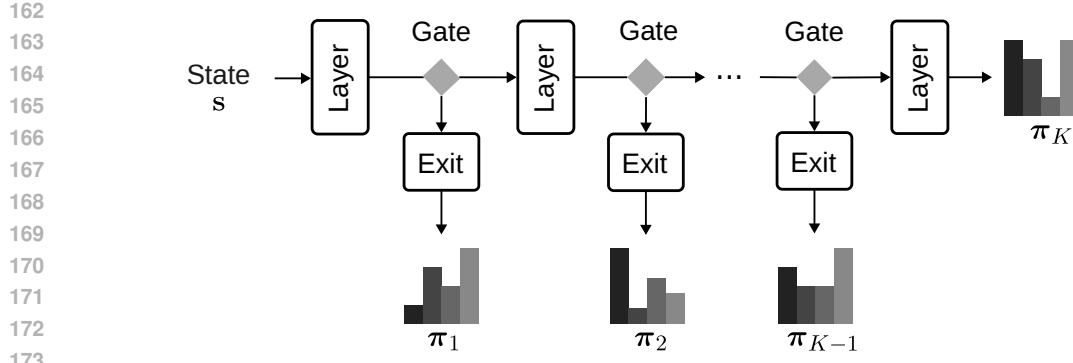


Figure 1: Example of an actor represented as an early exit neural network (ENN). The input state is processed layer-by-layer until a gate is reached. Based on a learned rule, a gate decides whether to terminate early or proceed with the computation. Each exit produces an action distribution for the current input state.

count factor that determines the importance of future rewards. We define the state-value function $V_\pi(s) = \mathbb{E}_\pi[G_t \mid s_t = s]$ to calculate the expected return following some policy π . Similarly, we define the action-value function $Q_\pi(s, a) = \mathbb{E}_\pi[G_t \mid s_t = s, a_t = a]$ as the expected return if first an initial action a is taken, after which the policy π is followed. Given an initial state distribution ρ_0 , the goal in RL is to find an optimal policy π^* that maximizes the expected return $\pi^* \in \arg \max_\pi \mathbb{E}_{s \sim \rho_0} [V_\pi(s)]$.

In deep reinforcement learning (DRL), policies and value functions are typically represented by deep neural network (NN): the policy (actor) π^θ with parameters θ , and the action-value function (critic) Q^ϕ with parameters ϕ . Actor-critic methods jointly learn both networks, where the policy typically maximizes an objective derived from the critic that is of the form $J_\pi(\theta; Q^\phi) = \mathbb{E}_{s \sim \mathcal{D}} [\mathbb{E}_{a \sim \pi_\theta(\cdot|s)} [Q^\phi(s, a)]]$, where \mathcal{D} is a replay buffer collecting states from interactions with the environment. Many state-of-the-art algorithms, such as SAC (Haarnoja et al., 2018) and TD3 (Fujimoto et al., 2018), are off-policy actor-critic methods, meaning they learn from data \mathcal{D} collected by past policies rather than requiring samples from the current policy.

4 METHOD

We now present our framework for integrating early exit neural network (ENN) into off-policy actor-critic methods. The approach is general and can be applied to any actor-critic method with minimal changes to the underlying architecture. We first introduce the early-exit actor architecture, then describe how exit selection is formulated as a budget-constrained resource allocation problem, and finally present the complete algorithm.

4.1 EARLY EXIT ACTOR

The key distinction in our approach is that we represent the actor as a deep ENN shown in Fig. 1. During the forward pass, data is propagated sequentially through the network layers. At each side branch, a gating policy decides whether to terminate the computation early. A stochastic gating rule is used instead of a deterministic one to encourage exploration during training and ensure that each exit is occasionally selected. If the gate activates, the corresponding early exit head is evaluated and its prediction is returned without subsequent layers being evaluated, thereby saving computation. Otherwise, the computation continues and the exit is not calculated. To reduce computational overhead, the gating function shares its hidden features with the actor.

We now formalize the architecture mathematically. First, we number the exits sequentially from earliest to last and denote the sub-policy at each exit by π_i for $i = 1, \dots, K$. Additionally, each exit before the final layer has a gate policy $g_i(\cdot \mid s) = \text{Bernoulli}(p_i(s))$, where p_i is a learned state-dependent probability parameter; sampling 1 indicates taking the exit, while 0 means resuming.

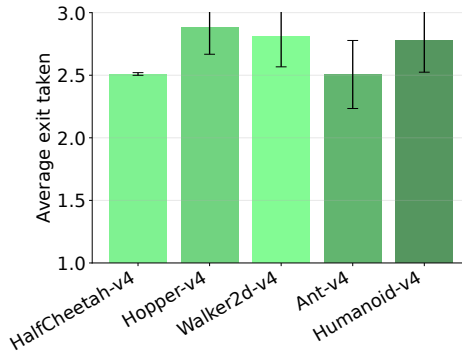


Figure 2: Average selected exit during soft actor-critic (SAC) training with greedy selection of exits based on learned Q-values. Results show the mean of the top five out of 200 agents per environment with one standard deviation. The early exit network has three branches $K = 3$. Without a resource constraint, later exits dominate.

Given a state s , the probability α that we terminate at exit $i = 1, \dots, K$ is given by

$$\alpha_i(s) := p_i(s) \prod_{j < i} (1 - p_j(s)), \quad (1)$$

assuming that we define $p_K(s) = 1$. The resulting policy π represented by the entire ENN is then a mixture of the exit policies

$$\pi(a | s) := \sum_{i=1}^K \alpha_i(s) \pi_i(a | s).$$

4.2 LEARNING BUDGET-AWARE EARLY EXIT ACTORS

We now discuss how to learn the gating policies g_i . In the supervised learning setting, ENNs typically rely on confidence-based exit rules such as measuring the entropy of the prediction, maximum class probability or patience, a criterion that exits once at least n consecutive predictions align (Xu & McAuley, 2023). These criteria are ill-suited for deep reinforcement learning (DRL), as high entropy drives exploration, which is crucial for success. Applying confidence-based methods steers behavior toward greedy action selection. Patience is also ineffective because DRL models are usually smaller than those in natural language processing (NLP) and offer much fewer exits. Such methods also introduce task-specific hyperparameters like thresholds that are difficult to tune.

In our reinforcement learning (RL) setting, each exit defines a policy π_i , and we can compare their performance directly using the expected value V_{π_i} . A natural idea is to pick the exit that maximizes the expected value in the current state, i.e., $\arg \max_i V_{\pi_i}(s)$. However, this approach tends to favor later exits, as they build upon the representations of previous layers and generally achieve higher returns. This intuition is supported by an experiment shown in Fig. 2, where later exits are selected disproportionately often, resulting in only minimal speedups. Moreover, this method provides little explicit control over the trade-off between performance and computational cost. Thus, we need to explicitly constrain the usage of later exits.

Optimal Budget-Aware Exit Selection. Different from approaches that rely on heuristics that are potentially hard to tune, we propose a principled approach that formulates early exit selection as a resource allocation problem. The key idea is that we maximize the expected value of the network’s actions while enforcing a hard budget constraint on inference costs.

We assume that each exit policy π_i has an associated Q-function Q_i . Given a state s , let $v = [Q_1(s, a_1), \dots, Q_K(s, a_K)]^\top$ with $a_i \sim \pi_i(\cdot | s)$ be an unbiased value estimate for each exit, and let $c = [c_1, \dots, c_K]^\top$ denote the per-exit costs, e.g., their floating point operations (FLOPs). For a

270 given budget $b \in \mathbb{R}$, we then solve the following linear program:
 271

$$272 \quad \alpha^* = \arg \max_{\alpha \in \mathbb{R}^K} \mathbf{v}^\top \alpha \quad (2a)$$

$$274 \quad \text{s.t.} \quad \mathbf{c}^\top \alpha \leq b, \quad \alpha \geq 0, \quad \mathbf{1}^\top \alpha = 1 \quad (2b)$$

276 The optimal weighting vector α^* denotes the optimal probability distribution over exit choices that
 277 maximizes the expected value while keeping the total cost within the budget. By rearranging Eq. 1
 278 we obtain the optimal probabilities p_i^* for each gate. The cost definition corresponds to the resource
 279 of interest, for example FLOPs with $c_i \propto \text{FLOPs}(\pi_i)$ though other choices are also possible. For
 280 our approach we decided to use normalized FLOP counts with $c_1 = 0$ and $c_n = 1$ and scale the
 281 intermediate costs linearly, while still satisfying $c_1 \leq c_2 \leq \dots \leq c_n$. The scalar budget b specifies
 282 a limit on the usable resources. With normalized costs $b \in [0, 1]$ becomes intuitive to scale. As b
 283 approaches zero, the gate favors earlier exits, while for b approaching one, the gate prefers the later
 284 exits. This yields a direct and tunable trade-off between speed and performance.

285 Lastly, we note that the linear program in Eq. 2 admits an efficient solution. Since K is small in
 286 practice, we can enumerate and evaluate the candidate extreme points quickly. For batches of states
 287 \mathbf{s} with corresponding \mathbf{Q} values, the computation parallelizes well on the GPU.

288 **The `BEXA` Training Objective.** Finally, we present the complete learning framework, which uses
 289 the optimal gate probabilities p_i^* as a supervisory signal. To keep our approach general, we assume
 290 that for a parameterized policy π^θ and critic Q^ϕ the underlying actor-critic algorithm provides an
 291 actor objective $J_{\text{actor}}(\theta; \pi^\theta, Q^\phi)$ that should be maximized with respect to the parameters θ .

292 For each exit policy π_i^θ , we learn a corresponding critic $Q_{\pi_i}^\phi$. Preliminary experiments indicated that
 293 maintaining a separate critic per exit substantially improved learning stability. Since the underlying
 294 method is off-policy, each critic can be learned from the same stream of data. To avoid the compu-
 295 tational cost of K separate critics, we use a single critic with shared features and K heads, one per
 296 exit, which adds only minor overhead. Importantly, we do not impose an early exit structure on the
 297 critic, which can lead to significant instability during training.

298 The final Budgeted EXit Actor (`BEXA`) method trains the complete early exit actor by optimizing an
 299 actor-critic objective J_{actor} and a gate loss $\mathcal{L}_{\text{gate}}$ at every exit. Thus, combined, we maximize the
 300 following objective for the actor:

$$302 \quad J_{\text{BEXA}}(\theta) = \sum_{i=1}^K \left(J_{\text{actor}}(\theta; \pi_i^\theta, Q_{\pi_i}^\phi) - \lambda \mathcal{L}_{\text{gate}}(\theta; p_i^\theta, p_i^*) \right).$$

303 The gate loss $\mathcal{L}_{\text{gate}}$ is a binary cross entropy loss between the predicted gate probabilities p_i^θ and the
 304 probabilities p_i^* obtained by solving the linear program from Eq. 2.

305 An illustrative pseudocode description of combining `BEXA` with SAC is provided in App. B.

310 5 EXPERIMENTS

312 To validate our proposed approach, Budgeted EXit Actor (`BEXA`), and to examine the efficiency
 313 of different design choices for employing early exit neural networks (ENNs) within actor-critic
 314 methods, we conduct two large-scale experiments based on soft actor-critic (SAC) (Haarnoja et al.,
 315 2018) and twin delayed deep deterministic policy gradient (TD3) (Fujimoto et al., 2018).

317 **Setup and Metrics.** For both SAC and TD3, we refer to their variants with budgeted early exits
 318 as `BEXA`-SAC and `BEXA`-TD3, respectively. Experiments are conducted on five MuJoCo (Todorov
 319 et al., 2012) tasks: Ant, Humanoid, Hopper, Walker2d and HalfCheetah. We report training curves
 320 with average return and actor inference speedups measured in floating point operations (FLOPs).
 321 Actors and critics are represented by two-layer MLPs with 256 units each and ReLU activation.
 322 For `BEXA` variants, we place an exit after every layer, yielding $K = 3$ exits in total. For each
 323 method-environment pair we run 200 hyperparameter configurations, where specifications are equal
 324 across methods where applicable. To minimize the effect of seed variance, we re-evaluate the top

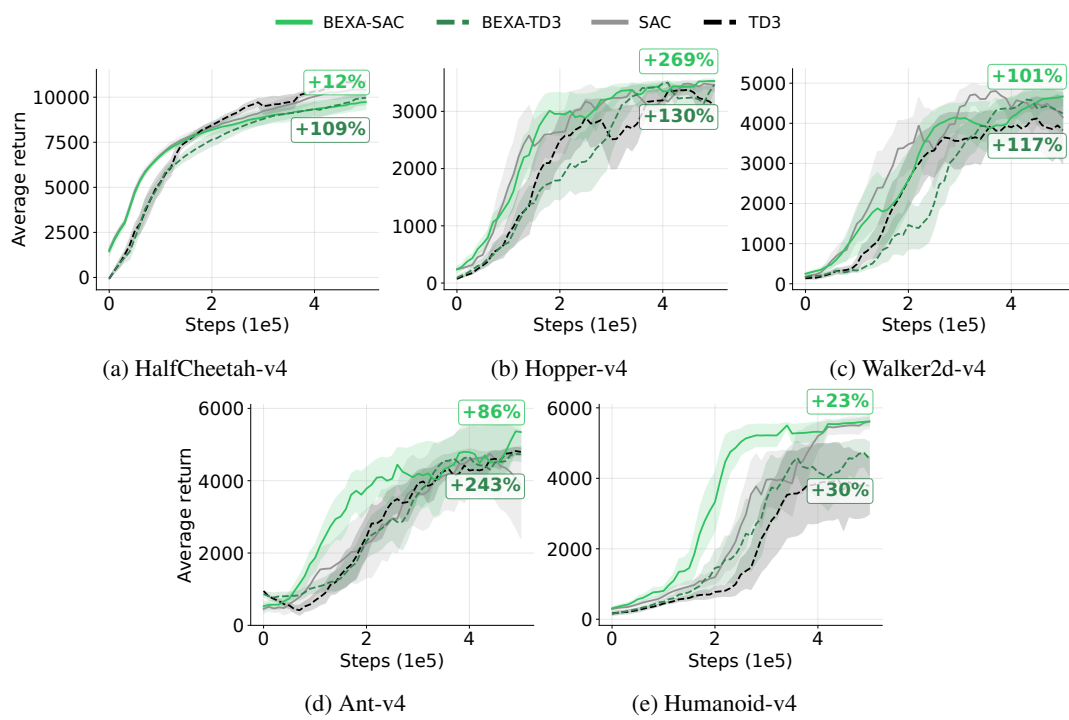


Figure 3: Training curves across MuJoCo tasks. We performed one evaluation run every 10000 environment steps. Curves are smoothed for readability and shaded with 0.5 standard deviation following Fujimoto et al. (2018). Green annotations indicate the average actor FLOP speedup of **BEXA** variants relative to their baselines over the *entire* training.

5 runs per sweep with two additional seeds, giving us three seeds in total, and select the best by mean return over the entire training. No further tuning was performed. Before averaging the return over multiple environments, we normalize the return per environment. This and more details are described in App. D.

Results. Results can be seen in Fig. 3. **BEXA** matches or exceeds the vanilla baselines, with notable gains on Ant and Humanoid. We hypothesize that these gains stem from a regularization effect of early exits as actor capacity is reduced. Despite introducing new hyperparameters, **BEXA** required no extra tuning budget relative to its baselines and the budget hyperparameter was straightforward to adapt. Using early exits can accelerate actor inference tremendously with speedups up to +269% while sampling in the environment, which accounts for a significant part of deep reinforcement learning (DRL) training. For more complex tasks such as Humanoid, the speedup diminishes as the entire network capacity is required to achieve high performance. However, using a more aggressive budget constraint can yield higher speedups, albeit at the expense of performance.

5.1 COMPARISON TO EARLY EXIT ALTERNATIVES

BEXA improves both performance and speed compared to its baseline methods. It still raises the question of how it compares to alternatives in the literature. As discussed in Related Work, direct comparison is difficult as research on early exit networks in DRL is limited, with most of the existing research being conducted in supervised learning. The approach that comes closest is that described in Kosta et al. (2022), which augments DQN (Hosu & Rebedea, 2016) with early exits, but it targets discrete action spaces, whereas SAC and TD3 use continuous ones. Other DRL acceleration methods, such as quantization and pruning, are orthogonal to our approach and can be combined with it. Benchmarking against these methods offers little insight, especially since methods such as quantization do not reduce FLOPs, but rather the type of operation.

	Method	Actor Speedup (\uparrow)		Mean Return (\uparrow)		Best Return (\uparrow)	
		SAC	TD3	SAC	TD3	SAC	TD3
381 382 383 384 385	Actor Inference	Backbone	1.0 \times	1.0 \times	36.2 \pm 5	33.6 \pm 6	64.1 \pm 16
		Ensemble	1.0 \times	1.0 \times	26.8 \pm 6	32.7 \pm 9	57.7 \pm 22
386 387 388 389 390 391	Exit Training	Imitate	1.18 \times	1.14 \times	29.2 \pm 7	34.0 \pm 10	65.9 \pm 23
	Gate Training	Advantage Softmax	1.164 \times 1.11 \times	1.179 \times 1.12 \times	58.3 \pm 12 50.3 \pm 16	40.5 \pm 12 49.3 \pm 11	99.2 \pm 14 98.7 \pm 18
392 393 394 395 396	Train Strategy	Stepwise	1.48\times	1.83\times	27.8 \pm 4	16.5 \pm 4	40.4 \pm 6
							42.4 \pm 23
		BEXA	1.3 \times	1.35 \times	62.8 \pm 17	38.7 \pm 12	101.2 \pm 13
							72.2 \pm 31

Table 1: Evaluation of alternative components for **BEXA** on MuJoCo using SAC and TD3. We report normalized returns, averaged over tasks and 3 seeds, with error bars indicating one standard deviation.

Instead, we propose baselines derived from early exit architectures in supervised learning, adapted to DRL. To our knowledge, these baselines have not been studied in DRL, though they have been effective elsewhere. We compare them in terms of performance, speed-up, and tuning effort.

Actor Inference. During sampling in the environment, we already employ the early exits of our actor to achieve speedups during training. Two alternative inference schemes are also worth considering: (i) always use the final (backbone) exit, which often achieves the best performance and (ii) form an ensemble over all exits as in Sun et al. (2021) leveraging the fact that each branch solves the same task. However, both require full actor inference and thus miss out on acceleration.

Exit Training. Instead of using the same loss for every head, we adapt another strategy inspired by self-distillation (Zhang et al., 2019). We train only the final exit (the backbone) with the standard objective and train all earlier exits to imitate its action distribution via an auxiliary imitation loss. This reduces critic complexity, as only one critic is needed for the backbone, but introduces a loss-scale imbalance between the normal loss and the imitation loss, which requires additional hyperparameters.

Gate Training. The exit criterion critically affects performance, as it has to reliably pick the best exit while balancing performance and speed for each state. As data sampling and learning are tightly coupled, wrong exiting can lead to catastrophic updates. Common heuristics from literature, such as maximum class probability, entropy thresholds and patience are ill-suited as previously discussed due to exploration and smaller model sizes. We consider:

1. *Advantage over backbone*: Taking the exits that have higher value over the backbone. This is similar to the strategy of taking the exit with maximum Q-value Kosta et al. (2022), but prefers earlier exits.
2. *Softmax over Q-values*: Instead of taking a maximum, we take a softmax over the distribution of Q-values per exit. A temperature hyperparameter controls greediness. This softmax defines the target decision distribution, which we map to gate probabilities via Eq. 1.

Importantly, in App. C we show that our optimal budget-aware exit selection approach allows for direct and intuitive control in the number of FLOPs by selecting an according hard budget constraint. This is significantly harder to achieve with the strategies mentioned above as ablations.

Training Strategy. We train all exits and gates simultaneously under a unified objective. Early exit architectures also allow for alternative training schemes. Following Kosta et al. (2022), we also evaluate a stepwise procedure that sequentially trains each exit branch while freezing the rest of the network, starting with the earliest exit until the final one.

432 **Setup.** For a fair comparison, all methods were given the same hyperparameter search budget.
 433 To better observe the effects of individual components, we drastically reduce network capacity to
 434 $4 - 16$ hidden units per layer. The best configurations are re-run to obtain three seeds per setting.
 435 Returns are normalized for each environment and then averaged across tasks. We compare speedups
 436 of actors in terms of FLOPs during the whole training. See Table 1 for results.
 437

438 **Results.** Using alternative actor inference yields no benefit: performance is similar for TD3 and
 439 worse for SAC, and it provides no speedup during training unlike the usage of early exits. The
 440 imitation-based training objective also underperforms. **BEXA**, which trains all heads using the un-
 441 derlying DRL loss, consistently achieves higher returns. Gate-training results are mixed. As ex-
 442 pected, for TD3 we observe higher returns as the greedier gating favors later exits, but at the cost
 443 of reducing speedup and making the performance-efficiency trade-off difficult. For SAC, **BEXA**
 444 improves both return and speed, suggesting that tighter budget constraints can also act as a form
 445 of regularization, boosting performance as well. Lastly, we observe that stepwise training performs
 446 poorly. It over-optimized for speedup at the expense of return, and training time increases drastically
 447 due to additional gradient steps per iteration. Finally, TD3 and SAC diverge substantially at very
 448 low actor capacity, we attribute this to a much narrower hyperparameter region.
 449

6 CONCLUSION

450 We introduced Budgeted EXit Actor (**BEXA**), a generic method for off-policy actor-critic methods
 451 that uses early exits in the actor to reduce the required number of computations under explicit budget
 452 constraints. To guarantee that the budget constraints are satisfied, we reformulate the exit selection
 453 as a resource allocation problem, which can be efficiently solved using linear programming. **BEXA**
 454 is straightforward to tune and matches or even outperforms vanilla baselines and adapted early exit
 455 alternatives from the literature across a range of tasks.
 456

457 **Limitations.** **BEXA** inherits some limitations common to early exit architectures. Training time
 458 can increase because all exits must be optimized. To circumvent this, asynchronous training archi-
 459 tectures could be used to amortize such costs by decoupling sampling from learning. Furthermore,
 460 dynamic branching makes efficient parallelization on GPUs challenging, a problem that affects the
 461 broader early exit community, not just deep reinforcement learning (DRL).
 462

463 **Future Work.** Despite these limitations, **BEXA** is widely applicable and can be used alongside
 464 other acceleration techniques, such as pruning, quantization, and distillation. Future work includes
 465 plans to integrate **BEXA** with additional reinforcement learning (RL) paradigms e.g. model-based
 466 RL and scaling to large neural network architectures like ResNets or Transformers (Farebrother
 467 et al., 2024), where the additional floating point operations (FLOPs) required by the gating mecha-
 468 nism will be negligible small. In spirit with Sutton’s “Bitter Lesson”, our aim is to provide general
 469 and efficient methods that leverage computation rather than task-specific heuristics, providing a
 470 practical foundation for faster and stronger DRL agents.
 471

REFERENCES

472 Konstantin Berestizshevsky and Guy Even. Dynamically sacrificing accuracy for reduced com-
 473 putation: Cascaded inference based on softmax confidence. In Igor V. Tetko, Vera Kurková,
 474 Pavel Karpov, and Fabian J. Theis (eds.), *Artificial Neural Networks and Machine Learning -*
 475 *ICANN 2019: Deep Learning - 28th International Conference on Artificial Neural Networks,*
 476 *Munich, Germany, September 17-19, 2019, Proceedings, Part II*, volume 11728 of *Lecture Notes*
 477 *in Computer Science*, pp. 306–320. Springer, 2019. doi: 10.1007/978-3-030-30484-3_26. URL
 478 https://doi.org/10.1007/978-3-030-30484-3_26.
 479

480 Steven Dalton and Iuri Frosio. Accelerating reinforcement learning through GPU atari em-
 481 ulation. In Hugo Larochelle, Marc’Aurelio Ranzato, Raia Hadsell, Maria-Florina Balcan,
 482 and Hsuan-Tien Lin (eds.), *Advances in Neural Information Processing Systems 33: Annual*
 483 *Conference on Neural Information Processing Systems 2020, NeurIPS 2020, December 6-12,*
 484 *2020, virtual*, 2020. URL <https://proceedings.neurips.cc/paper/2020/hash/e4d78a6b4d93e1d79241f7b282fa3413-Abstract.html>.
 485

486 Edanur Demir and Emre Akbas. Early-exit convolutional neural networks. *CoRR*, abs/2409.05336,
 487 2024. doi: 10.48550/ARXIV.2409.05336. URL <https://doi.org/10.48550/arXiv.2409.05336>.

488

489 Theresa Eimer, Marius Lindauer, and Roberta Raileanu. Hyperparameters in reinforcement learning
 490 and how to tune them. In Andreas Krause, Emma Brunskill, Kyunghyun Cho, Barbara Engelhardt,
 491 Sivan Sabato, and Jonathan Scarlett (eds.), *International Conference on Machine Learning, ICML
 492 2023, 23-29 July 2023, Honolulu, Hawaii, USA*, volume 202 of *Proceedings of Machine Learn-
 493 ing Research*, pp. 9104–9149. PMLR, 2023. URL <https://proceedings.mlr.press/v202/eimer23a.html>.

494

495

496 Lasse Espeholt, Hubert Soyer, Rémi Munos, Karen Simonyan, Volodymyr Mnih, Tom Ward, Yotam
 497 Doron, Vlad Firoiu, Tim Harley, Iain Dunning, Shane Legg, and Koray Kavukcuoglu. IMPALA:
 498 scalable distributed deep-rl with importance weighted actor-learner architectures. *CoRR*,
 499 abs/1802.01561, 2018. URL <http://arxiv.org/abs/1802.01561>.

500

501 Lasse Espeholt, Raphaël Marinier, Piotr Stanczyk, Ke Wang, and Marcin Michalski. SEED RL:
 502 scalable and efficient deep-rl with accelerated central inference. *CoRR*, abs/1910.06591, 2019.
 503 URL <http://arxiv.org/abs/1910.06591>.

504

505 Jesse Farnbrother, Jordi Orbay, Quan Vuong, Adrien Ali Taïga, Yevgen Chebotar, Ted Xiao, Alex
 506 Irpan, Sergey Levine, Pablo Samuel Castro, Aleksandra Faust, Aviral Kumar, and Rishabh Agar-
 507 wal. Stop Regressing: Training Value Functions via Classification for Scalable Deep RL, March
 508 2024. URL <http://arxiv.org/abs/2403.03950>. arXiv:2403.03950 [cs, stat].

509

510 Scott Fujimoto, Herke van Hoof, and David Meger. Addressing function approximation error in
 511 actor-critic methods. In Jennifer G. Dy and Andreas Krause (eds.), *Proceedings of the 35th Inter-
 512 national Conference on Machine Learning, ICML 2018, Stockholm, Sweden, July 10-15, 2018*, volume 80 of *Proceedings of Machine Learning Research*, pp. 1582–1591.
 513 PMLR, 2018. URL <http://proceedings.mlr.press/v80/fujimoto18a.html>.

514

515 Tuomas Haarnoja, Aurick Zhou, Pieter Abbeel, and Sergey Levine. Soft actor-critic: Off-policy
 516 maximum entropy deep reinforcement learning with a stochastic actor. *CoRR*, abs/1801.01290,
 517 2018. URL <http://arxiv.org/abs/1801.01290>.

518

519 Yizeng Han, Gao Huang, Shiji Song, Le Yang, Honghui Wang, and Yulin Wang. Dynamic neural
 520 networks: A survey. *CoRR*, abs/2102.04906, 2021. URL <https://arxiv.org/abs/2102.04906>.

521

522 Yizeng Han, Gao Huang, Shiji Song, Le Yang, Honghui Wang, and Yulin Wang. Dynamic neu-
 523 ral networks: A survey. *IEEE Trans. Pattern Anal. Mach. Intell.*, 44(11):7436–7456, 2022.
 524 doi: 10.1109/TPAMI.2021.3117837. URL <https://doi.org/10.1109/TPAMI.2021.3117837>.

525

526 Chris Hettinger, Tanner Christensen, Ben Ehlert, Jeffrey Humphreys, Tyler Jarvis, and Sean
 527 Wade. Forward thinking: Building and training neural networks one layer at a time. *CoRR*,
 528 abs/1706.02480, 2017. URL <http://arxiv.org/abs/1706.02480>.

529

530 Geoffrey E. Hinton, Oriol Vinyals, and Jeffrey Dean. Distilling the knowledge in a neural network.
 531 *CoRR*, abs/1503.02531, 2015. URL <http://arxiv.org/abs/1503.02531>.

532

533 Ionel-Alexandru Hosu and Traian Rebedea. Playing atari games with deep reinforcement learning
 534 and human checkpoint replay. *CoRR*, abs/1607.05077, 2016. URL <http://arxiv.org/abs/1607.05077>.

535

536 Gao Huang, Danlu Chen, Tianhong Li, Felix Wu, Laurens van der Maaten, and Kilian Q. Wein-
 537 berger. Multi-scale dense networks for resource efficient image classification. In *6th Inter-
 538 national Conference on Learning Representations, ICLR 2018, Vancouver, BC, Canada, April
 539 30 - May 3, 2018, Conference Track Proceedings*. OpenReview.net, 2018. URL <https://openreview.net/forum?id=Hk2aImxA>.

540 Adarsh Kumar Kosta, Malik Aqeel Anwar, Priyadarshini Panda, Arijit Raychowdhury, and
 541 Kaushik Roy. RAPID-RL: A reconfigurable architecture with preemptive-exits for efficient
 542 deep-reinforcement learning. In *2022 International Conference on Robotics and Automation, ICRA 2022, Philadelphia, PA, USA, May 23-27, 2022*, pp. 7492–7498. IEEE, 2022. doi: 10.1109/ICRA46639.2022.9812320. URL <https://doi.org/10.1109/ICRA46639.2022.9812320>.

546 Srivatsan Krishnan, Max Lam, Sharad Chitlangia, Zishen Wan, Gabriel Barth-Maron, Aleksandra
 547 Faust, and Vijay Janapa Reddi. Quarl: Quantization for fast and environmentally sustainable
 548 reinforcement learning. *Trans. Mach. Learn. Res.*, 2022, 2022. URL <https://openreview.net/forum?id=xwWsiFmUEs>.

551 Stefanos Laskaridis, Alexandros Kouris, and Nicholas D. Lane. Adaptive inference through early-
 552 exit networks: Design, challenges and directions. *CoRR*, abs/2106.05022, 2021. URL <https://arxiv.org/abs/2106.05022>.

555 Yann LeCun, John S. Denker, and Sara A. Solla. Optimal brain damage. In David S. Touretzky (ed.),
 556 *Advances in Neural Information Processing Systems 2, [NIPS Conference, Denver, Colorado, USA, November 27-30, 1989]*, pp. 598–605. Morgan Kaufmann, 1989. URL <http://papers.nips.cc/paper/250-optimal-brain-damage>.

559 Markus Nagel, Marios Fournarakis, Rana Ali Amjad, Yelysei Bondarenko, Mart van Baalen, and
 560 Tijmen Blankevoort. A white paper on neural network quantization. *CoRR*, abs/2106.08295,
 561 2021. URL <https://arxiv.org/abs/2106.08295>.

563 Michal Nauman, Mateusz Ostaszewski, Krzysztof Jankowski, Piotr Milos, and Marek Cy-
 564 gan. Bigger, regularized, optimistic: scaling for compute and sample efficient con-
 565 tinuous control. In Amir Globersons, Lester Mackey, Danielle Belgrave, Angela
 566 Fan, Ulrich Paquet, Jakub M. Tomczak, and Cheng Zhang (eds.), *Advances in Neu-
 567 ral Information Processing Systems 38: Annual Conference on Neural Information Pro-
 568 cessing Systems 2024, NeurIPS 2024, Vancouver, BC, Canada, December 10 - 15,
 569 2024*. URL http://papers.nips.cc/paper_files/paper/2024/hash/cd3b5d2ed967e906af24b33d6a356cac-Abstract-Conference.html.

571 Johan S. Obando-Ceron, Ghada Sokar, Timon Willi, Clare Lyle, Jesse Farebrother, Jakob Nico-
 572 laus Foerster, Gintare Karolina Dziugaite, Doina Precup, and Pablo Samuel Castro. Mixtures of
 573 experts unlock parameter scaling for deep RL. In *Forty-first International Conference on Ma-
 574 chine Learning, ICML 2024, Vienna, Austria, July 21-27, 2024*. OpenReview.net, 2024. URL
 575 <https://openreview.net/forum?id=X9VMhfFxwn>.

576 Haseena Rahmath P, Vishal Srivastava, Kuldeep Chaurasia, Roberto Gonçalves Pacheco, and Ro-
 577 drigo S. Couto. Early-exit deep neural network - A comprehensive survey. *ACM Comput. Surv.*, 57(3):75:1–75:37, 2025. doi: 10.1145/3698767. URL <https://doi.org/10.1145/3698767>.

581 Priyadarshini Panda, Abhroni Sengupta, and Kaushik Roy. Conditional deep learning for energy-
 582 efficient and enhanced pattern recognition. In Luca Fanucci and Jürgen Teich (eds.), *2016 De-
 583 sign, Automation & Test in Europe Conference & Exhibition, DATE 2016, Dresden, Germany,
 584 March 14-18, 2016*, pp. 475–480. IEEE, 2016. URL <https://ieeexplore.ieee.org/document/7459357/>.

586 Minh Pham, Minsu Cho, Ameya Joshi, and Chinmay Hegde. Revisiting self-distillation. *CoRR*,
 587 abs/2206.08491, 2022. doi: 10.48550/ARXIV.2206.08491. URL <https://doi.org/10.48550/arXiv.2206.08491>.

590 Simone Scardapane, Danilo Comminiello, Michele Scarpiniti, Enzo Baccarelli, and Aurelio Uncini.
 591 Differentiable branching in deep networks for fast inference. In *2020 IEEE International Con-
 592 ference on Acoustics, Speech and Signal Processing, ICASSP 2020, Barcelona, Spain, May
 593 4-8, 2020*, pp. 4167–4171. IEEE, 2020a. doi: 10.1109/ICASSP40776.2020.9054209. URL
<https://doi.org/10.1109/ICASSP40776.2020.9054209>.

594 Simone Scardapane, Michele Scarpiniti, Enzo Baccarelli, and Aurelio Uncini. Why should we add
 595 early exits to neural networks? *CoRR*, abs/2004.12814, 2020b. URL <https://arxiv.org/abs/2004.12814>.
 596

597 Tianxiang Sun, Yunhua Zhou, Xiangyang Liu, Xinyu Zhang, Hao Jiang, Zhao Cao, Xuanjing Huang,
 598 and Xipeng Qiu. Early exiting with ensemble internal classifiers. *CoRR*, abs/2105.13792, 2021.
 599 URL <https://arxiv.org/abs/2105.13792>.
 600

601 Surat Teerapittayanon, Bradley McDanel, and H. T. Kung. Branchynet: Fast inference via early
 602 exiting from deep neural networks. In *23rd International Conference on Pattern Recognition,
 603 ICPR 2016, Cancún, Mexico, December 4-8, 2016*, pp. 2464–2469. IEEE, 2016. doi: 10.1109/
 604 ICPR.2016.7900006. URL <https://doi.org/10.1109/ICPR.2016.7900006>.
 605

606 Emanuel Todorov, Tom Erez, and Yuval Tassa. Mujoco: A physics engine for model-based con-
 607 trol. In *2012 IEEE/RSJ International Conference on Intelligent Robots and Systems, IROS 2012,
 608 Vilamoura, Algarve, Portugal, October 7-12, 2012*, pp. 5026–5033. IEEE, 2012. doi: 10.1109/
 609 IROS.2012.6386109. URL <https://doi.org/10.1109/IROS.2012.6386109>.
 610

611 Abhishek Vashist, Sharan Vidash Vidya Shanmugham, Amlan Ganguly, and Sai Manoj P. D. DQN
 612 based exit selection in multi-exit deep neural networks for applications targeting situation aware-
 613 ness. In *IEEE International Conference on Consumer Electronics, ICCE 2022, Las Vegas, NV,
 614 USA, January 7-9, 2022*, pp. 1–6. IEEE, 2022. doi: 10.1109/ICCE53296.2022.9730182. URL
 615 <https://doi.org/10.1109/ICCE53296.2022.9730182>.
 616

617 Jue Wang, Ke Chen, Gang Chen, Lidan Shou, and Julian J. McAuley. Skipbert: Efficient inference
 618 with shallow layer skipping. In Smaranda Muresan, Preslav Nakov, and Aline Villavicencio (eds.),
 619 *Proceedings of the 60th Annual Meeting of the Association for Computational Linguistics (Volume
 620 1: Long Papers), ACL 2022, Dublin, Ireland, May 22-27, 2022*, pp. 7287–7301. Association
 621 for Computational Linguistics, 2022. doi: 10.18653/V1/2022.ACL-LONG.503. URL <https://doi.org/10.18653/v1/2022.acl-long.503>.
 622

623 Jiayi Weng, Min Lin, Shengyi Huang, Bo Liu, Denys Makoviichuk, Viktor Makoviychuk, Zichen
 624 Liu, Yufan Song, Ting Luo, Yukun Jiang, Zhongwen Xu, and Shuicheng Yan. Envpool: A highly
 625 parallel reinforcement learning environment execution engine. *CoRR*, abs/2206.10558, 2022.
 626 doi: 10.48550/ARXIV.2206.10558. URL <https://doi.org/10.48550/arXiv.2206.10558>.
 627

628 Canwen Xu and Julian J. McAuley. A survey on dynamic neural networks for natural language
 629 processing. In Andreas Vlachos and Isabelle Augenstein (eds.), *Findings of the Association for
 630 Computational Linguistics: EACL 2023, Dubrovnik, Croatia, May 2-6, 2023*, pp. 2325–2336.
 631 Association for Computational Linguistics, 2023. doi: 10.18653/V1/2023.FINDINGS-EACL.
 632 180. URL <https://doi.org/10.18653/v1/2023.findings-eacl.180>.
 633

634 Hongjie Zhang, Haoming Ma, and Zhenyu Chen. Fastact: A lightweight actor compression frame-
 635 work for fast policy learning. In *International Joint Conference on Neural Networks, IJCNN
 636 2023, Gold Coast, Australia, June 18-23, 2023*, pp. 1–8. IEEE, 2023. doi: 10.1109/IJCNN54540.
 637 2023.10191108. URL <https://doi.org/10.1109/IJCNN54540.2023.10191108>.
 638

639 Linfeng Zhang, Jiebo Song, Anni Gao, Jingwei Chen, Chenglong Bao, and Kaisheng Ma. Be
 640 your own teacher: Improve the performance of convolutional neural networks via self distillation.
 641 *CoRR*, abs/1905.08094, 2019. URL [http://arxiv.org/abs/1905.08094](https://arxiv.org/abs/1905.08094).
 642

643 Linfeng Zhang, Chenglong Bao, and Kaisheng Ma. Self-distillation: Towards efficient and compact
 644 neural networks. *IEEE Trans. Pattern Anal. Mach. Intell.*, 44(8):4388–4403, 2022. doi: 10.1109/
 645 TPAMI.2021.3067100. URL <https://doi.org/10.1109/TPAMI.2021.3067100>.
 646

647 Wangchunshu Zhou, Canwen Xu, Tao Ge, Julian J. McAuley, Ke Xu, and Furu Wei. BERT loses
 648 patience: Fast and robust inference with early exit. *CoRR*, abs/2006.04152, 2020. URL <https://arxiv.org/abs/2006.04152>.
 649

650 Wei Zhu. Leebert: Learned early exit for BERT with cross-level optimization. In Chengqing Zong,
 651 Fei Xia, Wenjie Li, and Roberto Navigli (eds.), *Proceedings of the 59th Annual Meeting of the*

648
649 *Association for Computational Linguistics and the 11th International Joint Conference on Natural*
650 *Language Processing, ACL/IJCNLP 2021, (Volume 1: Long Papers), Virtual Event, August 1-6,*
651 *2021, pp. 2968–2980. Association for Computational Linguistics, 2021. doi: 10.18653/V1/2021.*
652 *ACL-LONG.231. URL* [*https://doi.org/10.18653/v1/2021.acl-long.231*](https://doi.org/10.18653/v1/2021.acl-long.231).
653
654
655
656
657
658
659
660
661
662
663
664
665
666
667
668
669
670
671
672
673
674
675
676
677
678
679
680
681
682
683
684
685
686
687
688
689
690
691
692
693
694
695
696
697
698
699
700
701

702 **A USE OF LARGE LANGUAGE MODELS (LLMs)**
703

704 In accordance with ICLR authorship guidelines, we disclose our use of LLMs. GitHub Copilot and
705 ChatGPT were used to provide coding assistance, especially for plotting scripts, and for language
706 editing of the paper. They were also used to identify related work and compare alternative design
707 ideas. All methodological choices, experiments, and analyses were conducted by the authors.
708

709 **B PSEUDOCODE**
710

711 In Alg. 1 we provide pseudocode for Budgeted EXit Actor (**BEXA**) using soft actor-critic (SAC) as
712 an example. As stated before, **BEXA** is agnostic with respect to the underlying actor-critic method,
713 which we denote as the base in the algorithm description. The critic updates shown here correspond
714 to those used in SAC.
715

716 **Algorithm 1** Budgeted EXit Actor (**BEXA**)

717 **Require:** Off-policy base (e.g. SAC or TD3); budget b ; early-exit actor with exits $i = 1, \dots, K$;
718 sub-policies $\pi_i(\cdot | s)$; gates $g_i \sim \text{Bernoulli}(p_i^\theta(s))$; critics $Q_i^\phi(s, a)$
719 1: Initialize replay buffer \mathcal{D} , parameters θ, ϕ
720 2: **for** environment step $t = 1, 2, \dots$ **do** \triangleright **Act with early exits**
721 3: Observe s_t
722 4: **for** $i = 1..K$ **do**
723 5: Compute $p_i^\theta(s_t)$ and sample $g_i \sim \text{Bernoulli}(p_i^\theta(s_t))$
724 6: **if** $g_i = 1$ **then**
725 7: $a_t \sim \pi_i(\cdot | s_t)$; **break**
726 8: Step environment, observe (r_t, s_{t+1}, d_t)
727 9: Store $(s_t, a_t, r_t, s_{t+1}, d_t)$ in \mathcal{D}
728 10: **for** update step $u = 1, \dots, U$ **do** \triangleright **Learn from replay**
729 11: Sample minibatch $\mathcal{B} \subset \mathcal{D}$
730 12: **(1) Critic update (base-agnostic).** For each exit $i = 1..K$:
731 Compute a TD target $y_i^{(\text{base})}$ per the chosen off-policy base, e.g. for SAC:
732
$$y_i^{(\text{SAC})} = r + \gamma(1 - d) \mathbb{E}_{a' \sim \pi_i(\cdot | s')} \left[\min_{m \in \{1, 2\}} Q_{i,m}^{\bar{\phi}_m}(s', a') - \lambda \log \pi_i(a' | s') \right].$$

733 Then update ϕ by a gradient step on $\frac{1}{|\mathcal{B}|} \sum (Q_i^\phi(s, a) - y_i^{(\text{base})})^2$.
734 13: **(2) Linear program for exit mixture.**
735
$$\alpha^* = \arg \max_{\alpha \in \mathbb{R}^K} v^\top \alpha \quad \text{s.t.} \quad c^\top \alpha \leq b, \quad \alpha \geq 0, \quad \mathbf{1}^\top \alpha = 1$$

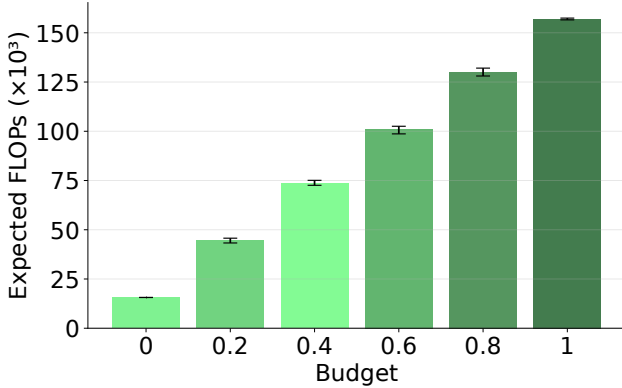
736 14: **(3) Map mixture to target gate probabilities.**
737 Using Eq. 1 to compute p^* recursively from α^* :
738
$$p_1^*(s) = \alpha_1^*(s), \quad p_i^*(s) = \frac{\alpha_i^*(s)}{\prod_{j < i} (1 - p_j^*(s))} \quad \text{for } i = 2, \dots, K.$$

739 15: **(4) Actor update (**BEXA** objective).**
740 16:
$$\theta \leftarrow \theta + \eta_\pi \nabla_\theta \frac{1}{|\mathcal{B}|} \sum_{s \in \mathcal{B}} J_{\text{BEXA}}(\theta; s, p^*)$$

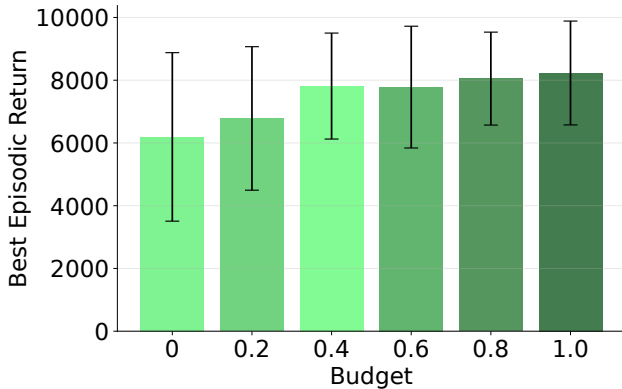
741
742
743
744
745
746
747
748
749
750
751
752
753
754
755

756 C EFFECT OF THE BUDGET ON COMPUTATIONAL COST AND RETURN
757

758 Here, we investigate how we can control the numbers of required floating point operations (FLOPs)
759 using our resource allocation formulation. In Fig. 4 we see how the expected FLOPs linear scale
760 with the normalized budget. Furthermore, Fig. 5 highlights that the performance increases with the
761 allowed budget.



776 Figure 4: Average FLOPs for the actor in relation of budget b when using BEXA-SAC. Evaluated
777 on the Halfcheetah-v4 environment using ~ 70 runs per bar. One standard deviation is plotted. This
778 shows that budget regulates flops explicitly and in a intuitive way.



794 Figure 5: Best Return reported for the actor in relation of budget b when using BEXA-SAC. Evaluated
795 on the Halfcheetah-v4 environment using ~ 70 runs per bar. One standard deviation is plotted.
796 Giving more budget allows for higher return.

797 D HYPERPARAMETERS
798

800 To follow best practices (Eimer et al., 2023), we list all relevant hyperparameters and search spaces
801 used in the experiments. For tuning the hyperparameters we used random search. For continuous
802 hyperparameters, we used q-log-uniform, which samples logarithmically and rounds to discrete
803 multiples of a step q .

805 In Tab. 2 and Tab. 3 we highlight the search spaces used for Fig. 3. For the ablation studies presented
806 in Tab. 1, we used the search spaces in Tab. 4 and Tab. 5. Furthermore, to facilitate comparison of
807 performance across environments, we normalize the return when aggregating results, see Tab. 6

810
811
812
813
814
815
816
817
818
819
820
821
822
823
824
825
826
827
828
829
830

Hyperparameter	Values / Range
batch_size	256
learning_starts	5000
policy_frequency	2
autotune	True
gamma	0.99
tau	q-log-uniform (min: 1e-3, max: 1e-2, q: 1e-3)
policy_lr	q-log-uniform (min: 1e-4, max: 7e-4, q: 1e-4)
q_lr	q-log-uniform (min: 3e-4, max: 1e-3, q: 1e-4)
gate_loss_scale	q-log-uniform (min: 1e-3, max: 1e-1, q: 1e-3)
budget	[0.0, 0.2, 0.4, 0.6, 0.8, 1.0]
actor_inference	early_exit
critic_kind	multi_head
actor_training	all_exits
gate_training	budget
training_scheme	jointly
total_timesteps	500000

Table 2: Hyperparameter configuration used for comparison of SAC and [BEXA](#)-SAC.

831
832
833
834
835
836
837
838
839
840
841

Hyperparameter	Values / Range
batch_size	256
learning_starts	25000
policy_frequency	2
gamma	0.99
tau	q-log-uniform (min: 1e-3, max: 1e-2, q: 1e-3)
lr	q-log-uniform (min: 1e-4, max: 1e-3, q: 1e-4)
policy_noise	[0.1, 0.2, 0.3, 0.4]
exploration_noise	[0.1, 0.2, 0.3]
noise_clip	[0.1, 0.2, 0.3]
gate_loss_scale	q-log-uniform (min: 1e-3, max: 1e-1, q: 1e-3)
budget	[0.0, 0.2, 0.4, 0.6, 0.8, 1.0]
actor_inference	early_exit
critic_kind	multi_head
actor_training	all_exits
gate_training	budget
training_scheme	jointly
total_timesteps	500000

Table 3: Hyperparameter configuration used for comparison of TD3 and [BEXA](#)-TD3.

858
859
860
861
862
863

864
 865
 866
 867
 868
 869
 870
 871
 872
 873
 874
 875
 876
 877
 878
 879
 880
 881
 882

Hyperparameter	Values / Range
batch_size	256
hidden_size	[4, 8, 16]
learning_starts	5000
policy_frequency	2
autotune	True
gamma	0.99
tau	q-log-uniform (min: 1e-3, max: 1e-2, q: 1e-3)
policy_lr	q-log-uniform (min: 1e-4, max: 7e-4, q: 1e-4)
q_lr	q-log-uniform (min: 3e-4, max: 1e-3, q: 1e-4)
imitate_loss_scale	q-log-uniform (min: 1e-2, max: 4e-1, q: 1e-2)
gate_loss_scale	q-log-uniform (min: 1e-3, max: 1e-1, q: 1e-3)
gate_loss_freq	[1, 2]
budget	[0.1, 0.2, 0.3, 0.4, 0.5, 0.6, 0.7, 0.8, 0.9]
gate_softmax_tmp	q-log-uniform (min: 1e-1, max: 2.0, q: 1e-1)
actor_inference	[early_exit, backbone, ensemble]
actor_training	[imitate, all_exits]
gate_training	[budget, adv, softmax]
training_scheme	[stepwise, jointly]
total_timesteps	500000

883
 884
 885
 886

Hyperparameter	Values / Range
batch_size	256
hidden_size	[4, 8, 16]
learning_starts	25000
policy_frequency	2
gamma	0.99
tau	q-log-uniform (min: 1e-3, max: 1e-2, q: 1e-3)
lr	q-log-uniform (min: 1e-4, max: 1e-3, q: 1e-4)
policy_noise	[0.1, 0.2, 0.3, 0.4]
exploration_noise	[0.1, 0.2, 0.3]
noise_clip	[0.1, 0.2, 0.3]
imitate_loss_scale	q-log-uniform (min: 1e-2, max: 4e-1, q: 1e-2)
gate_loss_scale	q-log-uniform (min: 1e-3, max: 1e-1, q: 1e-3)
gate_loss_freq	[1, 2]
budget	[0.1, 0.2, 0.3, 0.4, 0.5, 0.6, 0.7, 0.8, 0.9]
gate_softmax_tmp	q-log-uniform (min: 1e-1, max: 2.0, q: 1e-1)
kl_eps	q-log-uniform (min: 1e-1, max: 2.0, q: 1e-1)
actor_inference	[early_exit, backbone, ensemble]
actor_training	[imitate, all_exits]
gate_training	[budget, adv, softmax]
training_scheme	[stepwise, jointly]
total_timesteps	500000

906
 907

Table 5: Sweep configuration for BEXA-TD3 and alternative ablation components.

908
 909
 910
 911
 912
 913
 914
 915

Environment	Normalization (return)
HalfCheetah-v4	60.0
Walker2d-v4	30.0
Hopper-v4	30.0
Humanoid-v4	50.0
Ant-v4	40.0

916
 917

Table 6: Normalization constants used to scale returns for MuJoCo tasks.